Accepted Manuscript

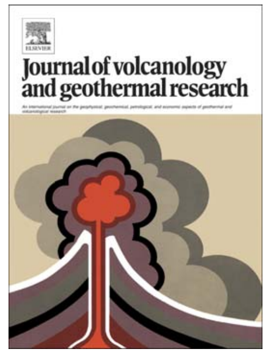

New insights into volcanic processes at Stromboli from Cerberus, a remote-controlled open-path FTIR scanner system

A. La Spina, M.R. Burton, R. Harig, F. Mure, P. Rausch, M. Jordan, T. Caltabiano

PII: S0377-0273(12)00280-6
DOI: doi: 10.1016/j.jvolgeores.2012.09.004
Reference: VOLGEO 4989

To appear in: *Journal of Volcanology and Geothermal Research*

Received date: 25 December 2011
Accepted date: 12 September 2012

Please cite this article as: La Spina, A., Burton, M.R., Harig, R., Mure, F., Rausch, P., Jordan, M., Caltabiano, T., New insights into volcanic processes at Stromboli from Cerberus, a remote-controlled open-path FTIR scanner system, *Journal of Volcanology and Geothermal Research* (2012), doi: 10.1016/j.jvolgeores.2012.09.004

New insights into volcanic processes at Stromboli from Cerberus, a remote-controlled open-path FTIR scanner system

La Spina A.[a], Burton M.R.[b], Harig R.[c,d], Mure F.[a], Rausch P.[c], Jordan M.[c], Caltabiano T[a].

[a] Istituto Nazionale di Geofisica e Vulcanologia, Osservatorio Etneo, Catania, Italy

[b] Istituto Nazionale di Geofisica e Vulcanologia, Pisa, Italy

[c] TUHH, Technical University of Hamburg-Harburg, Hamburg, Germany

[d] Bruker Optics, Germany

Abstract

The ordinary, low intensity, activity of Stromboli volcano is sporadically interrupted by more energetic events termed, depending on their intensity, “major explosions” and “paroxysms”. These short-lived energetic episodes represent a potential risk to visitors to the highly accessible summit of Stromboli. Observations made at Stromboli over the last decade have shown that the composition of gas emitted from the summit craters may change prior to such explosions, allowing the possibility that such changes may be used to forecast these potentially dangerous events.

In 2008 we installed a novel, remote-controlled, open-path FTIR scanning system called Cerberus at the summit of Stromboli, with the objective of measuring gas compositions from individual vents within the summit crater terrace of the volcano with high temporal resolution and for extended periods. In this work we report the first results from the Cerberus system, collected in August-September 2009, November 2009 and May-June 2010.

We find significant, fairly consistent, intra-crater variability for CO_2/SO_2 and H_2O/CO_2 ratios, and relatively homogeneous SO_2/HCl ratios. In general, the southwest crater is richest in CO_2, and the northeast crater poorest, while the central crater is richest in H_2O. It thus appears that during the measurement period the southwest crater had a somewhat more direct connection to a primary, deep degassing system; whilst the central and northeast craters reflect a slightly more secondary degassing nature, with a supplementary, shallow H_2O source for the central crater, probably related to puffing activity. Such water-rich emissions from the central crater can account for the lower crystal content of its eruption products, and emphasise the role of continual magma supply to the shallowest levels of Stromboli's plumbing system.

Our observations of heterogeneous crater gas emissions and high H_2O/CO_2 ratios do not agree with models of CO_2-flushing, and we show that simple depressurisation during magma ascent to the surface is a more likely model for H_2O loss at Stromboli. We highlight that alternative explanations other than CO_2 flushing are required to explain distributions of H_2O and CO_2 amounts dissolved in melt inclusions.

We detected fairly systematic increases in CO_2/SO_2 ratio some weeks prior to major explosions, and some evidence of a decrease in this ratio in the days immediately preceding the explosions, with periods of low, stable CO_2/SO_2 ratios between explosions otherwise. Our measurements, therefore, confirm the medium term (~weeks) precursory increases previously observed with MultiGas instruments, and, in addition, reveal new, short-term precursory decreases in CO_2/SO_2 ratios. immediately prior to the major explosions. Such patterns, if shown to be systematic, may be of great utility for hazard management at Stromboli's summit.

Our results suggest that intra-crater CO_2/SO_2 variability may produce short-term peaks and troughs in CO_2/SO_2 time series measured with in-situ MultiGas instruments, due simply to variations in wind direction.

Keywords OP-FTIR scanning system; Stromboli Volcano; Explosive activity

1. Introduction

Stromboli volcano, in the Aeolian island arc (figure 1a), is known as the "Lighthouse of the Mediterranean" for its regular (~every 10-20 min) explosive activity, launching crystal-rich black scoriae to 100-200 m height (Rosi et al., 2000) constituting a rich and impressive spectacle for both volcanologists and tourists from every part of the world. Stromboli island (924 m asl) is the emerged upper part of ~3-km-high stratovolcano erupting a volatile-rich high-potassium (HK) arc basalt (Métrich et al., 2001; Bertagnini et al., 2003, 2008) over the past 1400 years in the Tyrrhenian Sea (figure 1b).

Stromboli's normal explosive activity is focussed on vents within an elliptical crater terrace area 750 m a.s.l. (figure 1c), and is driven by the bursting of gas slugs that form by gas coalescence at depths of between 1 and 3 km beneath the terrace crater (Burton et al., 2007a). This "ordinary" strombolian activity is sporadically interrupted by more energetic events termed major explosions for typical energetic explosions and paroxysms for the most powerful examples (Barberi et al., 1993). Both types of events can produce brownish to yellow pumice clasts (know as golden pumice) sourced from a deeper, gas-rich, low porphyritic magma (Bertagnini et al., 2003; Métrich et al., 2005).

Stromboli has been for many years a laboratory volcano for studying magmatic degassing process (Allard et al., 2008), and significant recent advances in geochemical gas monitoring have taken place, with automatic measurements of SO_2 flux (Burton et al., 2009) and CO_2/SO_2 ratio (Aiuppa et al., 2011). Open-path FTIR (OP-FTIR) measurements (Oppenheimer et al., 1998) have been sporadically carried out on Stromboli, using the hot crater vents and scoria as a radiation source. OP-FTIR is an increasingly used technique in volcanology, capable of measuring multiple gas species in a variety of configurations, allowing fast processes to be investigated (Allard et al., 2005; Burton et al., 2007a), gas fluxes to be measured (Duffell et al., 2001) and total gas compositions to be determined (Burton et al., 2000) when used with appropriate absorption spectrum retrieval techniques (e.g. Burton, 1999).

In this paper we present time series of the gas phase composition emitted from three separate active vents in the northeast crater (NEC), central crater (CC) and southwest craters (SWC) (figure 1c). These measurements were performed with the Cerberus system, a novel, remote-controlled continuously measuring open-path FTIR spectrometer. We report gas composition data collected during quiet background activity in September 2009, and a few days prior to two major explosions which occurred on 24 November 2009 and 25 June 2010. Volcanological descriptions of these explosions were reported by Andronico and Pistolesi (2010) and La Felice and Landi (2011).

2. Cerberus system

Cerberus is a multi-component integrated remote sensing system whose purpose is to automatically measure the chemical composition of gas emitted by individual craters of Stromboli volcano. The system is positioned close to the summit of Stromboli looking down into the crater terrace, on Pizzo sopra La Fossa 900 m a.s.l (figure 1c). Cerberus (figure 2) consists of three main components (hence its name, after the mythological three-headed dog which guards the gates of Hades): an FTIR spectrometer (Midac Corp, Irvine, CA, USA, http://www.midac.com), an azimuth-elevation scanning system to align the field of view of the interferometer, and an infrared camera (FLIR Photon 320). The scanning system is capable of steering light from a 57°×45° field of view into the interferometer. The FTIR spectrometer (M4406-S) allows measurements with a maximum spectral resolution of 0.5 cm^{-1}. It is equipped with a 4-stage Peltier-cooled MCT detector sensitive between 2000 and 5000 cm^{-1}, allowing measurements to be performed without liquid nitrogen. The field of view of the instrument is 20 mrad, producing an imaging area at the ~300 m range of the summit craters of ~6 m.

All components are enclosed in an O-ring-sealed aluminium box ensuring maximum protection from volcanic acid gases. Two infrared transparent windows allow radiation to reach the camera and scanner/FTIR, the smaller with a 3 cm diameter is made of germanium and it is used by the infrared camera, whereas the other, made from sapphire, with a 15 cm diameter, illuminates the spectrometer (figure 2b). The system is controlled by an integrated imaging and spectroscopy software. The view of the crater area, recorded by the infrared camera, is displayed in real-time and the software permits the alignment of the field of view of the spectrometer to any position within the infrared image. The software also controls the interferometer, records the interferograms and performs the Fourier transforms. Both, interferograms and images of the infrared camera are stored for later analysis. The software runs on an internal 3.5’’ mini-PC by Kontron (www.kontron.com) under Microsoft Windows XP (figure 2c). The system is connected via a Wi-Fi network from the summit of Stromboli down to the local INGV observatory, allowing direct control using remote desktop software. The instrument is unique and novel, being the first fully remote controlled integrated scanner/infrared camera/OP-FTIR operation in a volcanic environment. The ability via remote control to simply click on an area of interest and measure the infrared spectrum from that exact point is a step-change in terms of flexibility and ease of use for volcanic remote sensing. It also opens the possibility of developing automatic programs of measurements in which specific areas are measured routinely in a cycle.

The raw data produced by the OP-FTIR system are infrared spectra, which require analysis for the determination of gas path amounts. Gas path amounts are used rather than gas concentrations because the exact distribution of gases along the path between the radiation source (hot volcanic rock) and the spectrometer is unknown. We report the gas path amounts in units of molecules.cm^{-2}, produced by assuming a path length of 1 cm multiplied with an average concentration in molecules.cm^{-3}.

The retrieval of quantitative gas amounts from measured absorption spectra is performed using a retrieval scheme developed from Burton (1999). The forward model in this scheme uses a radiative transfer model (Reference Forward Model, available at http://www.atm. ox.ac.uk/RFM) and the HITRAN08 molecular spectroscopic database (Rothman et al., 1998). Optimal estimation is used to iterate to the best fit (Rodgers, 2000).

2.1 Real-world use of the Cerberus instrument

The Cerberus instrument is complex and works in a highly challenging environment on the border of Stromboli's craters, where it suffers a variety of hardships including exposure to acid-rich gases, ash falls, large diurnal temperature variations and occasional heavy rains. The system is protected by a surrounding box structure which is covered in rocks, reducing exposure to direct sunlight and rain. The attention given to sealing the instrument box itself has resulted in virtually no infiltration of acid gases within the instrument, notwithstanding the harsh environment. However, the sapphire window through which infrared radiation passes was rapidly attacked by acid gases and ash fall, necessitating frequent cleaning and replacement of the window.

The ability to run the instrument remotely greatly facilitated measurement collection. While in theory an automatic data collection approach could be utilised, in practice we performed all measurements manually, thereby guaranteeing the data quality. Data collection is not always simple, as small changes in the orientation of the mirror can produce either observations of hot gas against a cool background, and therefore hard-to-analyse gas emission spectra, or more tractable absorption spectra, which are obtained when cooler gas is observed in front of a hotter background. Trial and error is the only way to find the optimal positioning, which changes frequently as the activity changes and crater morphology evolves.

We were concerned that while we point at one crater vent we might be also measuring gas emissions from other vents which drift into the observation line. If the 'contaminating' gases were of similar abundance to the target vent this would obviously have a detrimental effect on our ability to distinguish distinct gas compositions from different source. The occasions when this might be a problem were when the plume was carried directly towards the instrument, but on these occasions measurements were not performed as visibility was poor. In general we found a high degree of fidelity in terms of cross-talk between gas compositions from different craters, as demonstrated in figure 3.

Explosions sometimes produce an unexpected effect in our 4-stage Peltier cooled MCT detector; it appears that the sharp burst of intense IR radiation focussed on the detector was sufficient to heat it slightly, reducing the efficiency of the detector and producing a reduction in observed intensity.

This quickly recovered however, and allowed the explosive gas to be well-measured some seconds after the explosion.

The weight of the Cerberus instrument is 18 kg, which allowed it to be carried with an open-frame rucksack up to the summit area and back to the observatory when maintenance was required.

3. Results

The analysis of infrared spectra collected in passive mode produced path amounts of the following species: SO_2, CO_2, H_2O and HCl. The molar ratios of volcanic plume are obtained (figure 4) plotting the relative gas amounts against retrieved SO_2 in a scatter plot, and fitting a simple y=mx+c line where *m* represents the molar ratio of the two species (x and y) and c the background atmospheric amount if they are present both in the plume and the atmosphere (e.g. H_2O and CO_2). Therefore, we have determined the H_2O/SO_2, CO_2/SO_2, and HCl/SO_2 ratios characterizing the passive degassing which is between explosive episodes of "ordinary" activity (figure 5). All ratios and % compositions reported in this paper are in molar units.

In table 1 we report the CO_2/SO_2, H_2O/CO_2 and HCl/SO_2 ratios of gas phase emitted by active vents with their relative standard deviation (*se*) for each interval considered.

From 28 August to 14 September 2009, data were collected primarily from the NEC. For the 17 and 19 November 2009 we report the gas phase composition of all three vents. For 12 and 24 November 2009 we have data from only CC vent and for 16 and 26 November only from NEC, whilst for the other days we collected data from both NEC and SWC vents (table 1). Prior to the 25 June 2010 major explosion, with the exception of 11 and 17 June when we measured the SWC, data were collected primarily from the NEC.

In figure 4 we present the gas molar ratios from all three craters for 19 November. Examining the HCl vs SO_2 scatter plot we observe a similar amount of HCl but a relative higher content of SO_2 in the NEC phase (with a HCl/SO_2 of ~0.6) respect to SWC and CC vents, that shows a very similar HCl/SO_2 ratio of ~ 0.7.

We note that each crater has a different value of intercept point in CO_2 vs SO_2 and H_2O vs SO_2 scatter plots reflecting the different pathlength between the measured vent and Cerberus, with NEC being the furthest away at ~300 m, then SWC at ~270 m and finally CC at ~240 m distance. The NEC and CC gas results are characterized by a similar CO_2/SO_2 ratio (~6) but lower with respect to SWC (~9). H_2O vs. SO_2 plots (figure 4a) demonstrate that the CC gas phase is richer in H_2O with respect to the other vents. This observation is supported by H_2O/CO_2 ratios from all three periods considered (table 1), in which the CC showed a ratio >15, whilee the NEC and SWC are characterized by a ratio of less than 10. After the 24 November 2009 major explosion, we observed a higher value of H_2O/CO_2 in NEC, similar that seen at the CC.

Considering the first interval (table 1a), on “ordinary” activity of Stromboli, we observed a systematically heterogenous composition between the active vents, with the SWC gas phase containing higher values of CO_2/SO_2 (>5) while the NEC and CC together have lower and rather similar CO_2/SO_2 values of around 3.

During the second period (table 1b) we have information before and after the major explosion which occurred on 24 November 2009. We observe again a relatively higher value of CO_2/SO_2 ratio at the SWC of 9 with respect to the other vents. Moreover, CO_2/SO_2 ratios show a progressively increasing trend in all three crater before the major explosion; this increase is more evident in NEC emission (from 2 on 16 November to ~ 6 on 20 November). On 20 November, four days before the major explosion, we observe a decrease in CO_2/SO_2 ratio in gas phase of SWC vent. After the 24 November explosive event, gases emitted from NEC and CC shows a lower CO_2/SO_2 ratio than that observed before the explosive episode and very close to the value of the “ordinary” activity, reported in table 1a.

In the third period (table 1c) we observed a strong increasing trend in CO2/SO2 ratios at the NEC prior to the 25 June 2010 major explosion. In figure 5 we summarize the CO_2/SO_2, HCl/SO_2 and H_2O/CO_2 ratios of gas phase emitted by active vents in all three intervals considered.

4. Discussion

Our results provide new insights into magma-gas dynamics at Stromboli, and suggest new explanations for previously observations. In this discussion we will investigate five distinct volcanic processes controlling Stromboli's activity, by examining the implications of a heterogeneous intra-crater gas composition, and proposing a new schematic model of Stromboli's. plumbing system. In detail, we discuss the connection between water-rich gas emissions from the central crater and propose a likely connection with shallow degassing puffing behaviour (section 4.1, figure 6). We then focus on the impact of water-rich gas emissions from the central crater on crystal formation of eruption products, and suggest a volatile-composition driven explanation for the observed differences in porphyricity of those products (section 4.2). Moreover, we explain why magma dehydration from deep CO_2 flushing at Stromboli is inconsistent with our observations, and highlight the need for an alternative explanation for the observed distribution of melt inclusion compositions (section 4.3). Then we compare our measurements with those from MultiGas, and highlight the potential importance of intra-crater gas heterogeneity for the interpretation of in-situ measurements of plume gas composition on Stromboli (section 4.4, figure 7). Finally, we investigate the significance of our results in terms of forecasting major explosions, and implications for current models of the major explosion source mechanism (section 4.5).

4.1 New insights into the plumbing system of Stromboli

Our results show, for the first time, that there is evidence for significant heterogeneity in gas composition in space as well as time within Stromboli's crater terrace. Such spatial heterogeneity is presumably controlled by both the geometry of the magma feeding system and magma dynamics, in a similar manner to that observed at the craters of Mt. Etna (Burton et al., 2003; La Spina et al., 2010). We observe a trend of decreasing CO_2/SO_2 ratio going from southwest to northeast across the crater terrace, and a peak in H_2O emissions from the central crater. CO_2/SO_2 ratios are controlled primarily by SO_2 degassing, as the vast majority of CO_2 is already in the gas phase within the edifice of Stromboli, thanks to its low solubility in silicate liquids (Papale, 1999).

We note that no realistic variation in oxidation state of magma during ascent (Burgisser and Scaillet, 2006) can appreciably affect the CO_2 content of the gas emission, as the CO_2/CO ratio remains strongly in favour of CO_2. Sulphur may be emitted as H_2S, which is challenging to measure with OP-FTIR due to its weak infrared absorption band, but this species has not been measured in significant quantities with the H_2S chemical sensor within the MultiGas instrument on Stromboli (Allard et al., 2000; Aiuppa et al., 2005). We can therefore, safely use the CO_2/SO_2 ratio as a robust indicator of magma chemistry and gas dynamics.

Gas transport within Stromboli is complex, and plays a determining role in the persistent activity of the volcano. The interpretative framework for our observations of degassing from Stromboli comes from the model of closed- and open-system degassing proposed by Burton et al. (2007). The volatile-rich magma which feeds Stromboli ascends in quasi-closed system until it becomes sufficiently vesiculated to allow open system degassing at a pressure of between 50 and 100 MPa, when gas can ascend faster than the magma. Magma continues to ascend and degas after this point, and therefore we observe at the surface a superposition of gas rising from the point of transition from closed to open-system degassing with gas produced from the entire magma column. The CO_2 flux is generated solely from the point of transition to open-system, as there is negligible CO_2 release from the magma column, which has previously lost the vast majority of its CO_2. Overall changes in CO_2/SO_2 ratios in the bulk plume are therefore controlled by changes in magma supply to the open-system transition, changes in the depth of this transition and magma circulation within the conduit. In other words variations in CO_2/SO_2 between craters reflect on the balance between magma supply to the open-system transition point and magma supply to the surface. The higher the CO_2/SO_2 ratio the stronger is the link to the deeper source, and the relatively reduced role of gas escape from shallower magmas. On the contrary, lower CO_2/SO_2 ratios reflect a weaker connection to the deep supply and stronger contribution from magma degassing within the shallow conduit system.

A picture of the Stromboli's plumbing system may become more clear from the our observations of the decreasing CO_2/SO_2 compositions across the crater terrace. Our findings indicate that the SWC is connected to a deep supply, while the CC and NEC are progressively more closely coupled with shallower degassing. This suggests a branched magmatic system with the main deep conduit towards the SW and branching at some depth towards the northeast. Following La Spina et al. (2010), the possible branching depth can be constrained combining gas flux and composition measurement from each crater, as was done on Etna. For Stromboli we currently have only the bulk SO_2 fluxes available however, based on S solubility models from SolEx (Witham et al., 2011) during open-system degassing, we can propose that the branch must have a minimum depth constrained to be where sulphur is 50-70% degassed, as the typical CO_2/SO_2 ratio at SWC is between 50 and 100% greater than that at the CC and NEC. Such a fractionation would be impossible to achieve if most S were already exsolved. Moreover, considering the S solubility, SO_2 degassing of 50-70% occurs at 30-40 MPa, or 1.0-1.3 km depth, therefore we can propose that it is at this depth that the branching between SWC and CC-NEC takes place.

A relatively large volume of very shallow degassing magma source is required to explain the excess H_2O emissions at the CC. H_2O continues to degas even at atmospheric pressure (Witham et al., 2011), and therefore a peak in H_2O emissions from the CC, in the absence of excess SO_2 emissions, can best be explained by a shallow magma body 'boiling', that is, degassing almost pure H_2O. This gas flux will be overlaid on the background degassing fed from depth which is evidenced by the significant CO_2 release from the CC.

Supporting evidence for the presence of a shallow magma reservoir immediately beneath the summit craters comes from the volcanological observation of the rapid outpouring of ~1 million m3 of lava at the start of both the 2002/03 and 2007 eruptions of Stromboli (Landi et al., 2006 and 2007). Such a shallow magma accumulation zone may produce behaviour similar to that seen at lava lakes, where a proportion of degassing takes place quiescently from the entire surface of the lake, while a more vigorous degassing occurs at a single location which can move with time (Oppenheimer et al., 2009). This may be the source of the observed 'puffing', which occurs preferentially via the CC and NEC craters and more rarely from the SWC (Landi et al., 2011). We use this puffing distribution to complete our schematic model of the Stromboli plumbing system constrained by our data as shown in figure 6.

An implication of this interpretation is that puffing is not coupled with a deep degassing process, but is controlled instead in by the rate of magma supply and removal from the shallow reservoir. It is therefore unlikely to be a useful indicator of processes which occur at depth and which drive the more explosive phenomena observed at Stromboli. On the contrary puffing should be strongly linked with the degassing of the least soluble gases such as HCl, and further work on investigating the coupling between HCl gas release and shallow magma dynamics revealed by puffing should be carried out.

A further implication of the observation of excess H_2O degassing at the CC, is that it requires a continuous supply of degassing magma to the uppermost portion of the plumbing system. It has been suggested by Métrich et al. (2010) that magma convection may occur instead only up to the base of the 3 km tall volcanic edifice, a model which is not supported by our observations, which requires continuous magma supply to the upper reservoir, above the proposed branching point, to produce the continual H_2O and HCl fluxes.

Indeed, our data challenge the idea of a deep limit for magma convection at Stromboli (Mètrich et al., 2010), as this would produce a homogeneous gas composition from all craters, as opposed to the quite heterogeneous gas composition that we observe.

Finally, our results shed some indirect light on the question of what proportion of degassing occurs via puffing. We see in figure 4 that the absolute concentrations of volcanic gas species are rather similar for each of the crater measurements. In the case of a total gas flux dominated by puffing then the puffing crater (in this case the CC) should have a much larger concentration than that released from the other craters. Instead, we observe a rather equal distribution of gas from each of the three craters, suggesting that the gas emission from the CC is approximately one third of the total gas flux, and therefore within the range (2 - 45%) estimated by Harris and Ripepe (2007).

4.2 Impact of water-rich degassing on eruption product porphyricity

At any given depth the amount of water dissolved in the melt is proportional to the water fugacity (Dixon et al., 1999), which at low pressures approximates closely to the partial pressure of water. Variations in the H_2O/CO_2 ratio therefore affect the partial pressure of H_2O and the concentration of H_2O dissolved in the melt. Our observations show that the CC is systematically richer in water compared with both the other craters, and therefore the melt in the CC will be consequently enriched in dissolved H2O. Gas compositions for two typical days from each crater are as shown in table 2. The typical molar abundance of H_2O in the CC is 95%, compared with 85% in the SWC and NEC. This ~10% difference in H_2O partial pressure will result in a ~10% higher H_2O content for melts residing in the CC.

Landi et al. (2011) reported detailed and valuable information on the heterogeneity of eruption products from Stromboli's craters, collected between 2005 and 2008. They discovered a modest but systematically lower crystal content in products from the CC compared with the other craters. There are two main ways to explain this observation. The crystal content heterogenity may arise due to a difference in temperature or due to a difference in H_2O content of the melt. Landi et al. (2011) assumed that the gas composition would be identical at each crater, and therefore proposed that temperature differences best explain the heterogeneous products. Our observations demonstrate instead that the H_2O content of the CC melts will be 10% higher than that in the other craters, and since crystallisation is strongly coupled with H_2O content in basaltic melts this higher H_2O will produce a systematically lower crystal content in the CC products in agreement with the observations reported by Landi et al. (2011). It is particularly striking to compare the Cerberus results from November, when gas compositions were measured at each crater on two different days, with figure 4 from Landi et al. (2011) . There is a clear match between the gas compositions and the crystal content. We therefore propose that it is the gas composition heterogeneity which drives the eruption product heterogeneity. Low pressure experiments aimed at studying the isothermal relationship between crystal content and dissolved water contents of natural Stromboli samples would allow this hypothesis to be tested.

4.3 The role of CO_2 gas flushing at Stromboli

Measurements of H_2O and CO_2 contents of melt inclusions trapped in crystals from various pressures at Stromboli do not fit readily onto simple degassing paths, but are instead clouds of data points, with little systematic variability (Mètrich et al., 2010). It has become common to attempt to explain this cloud by invoking a CO_2 flushing process, whereby excess CO_2 flushes melts at high pressures and, due to the relative decrease in H_2O fugacity, induces a release of H_2O (Mètrich et al., 2010; Aiuppa et al. 2010). Theoretically, such a process explains the observed variation in MI composition very well. However, the CO_2 flushing process is invoked without defining the source or the destiny of the CO_2, in the context of a steady state system. Clearly, the CO_2 invoked in flushing must also degas from the system, allowing direct testing of the CO_2 flushing hypothesis. Our observations allow us to carry out this test.

Firstly we emphasise that if excessive H_2O loss were occurring at depth due to CO_2 flushing then there would be little heterogeneity in H_2O emissions between craters, as the bulk of this species would have been exsolved well below the relatively shallow branching implied by the summit crater CO_2/SO_2 emissions (figure 6). Instead we observe a significant heterogeneity in the H_2O content of gas emissions.

Secondly, we can calculate the amount of CO_2 required to produce significant dehydration between 100 and 200 MPa, and examine whether this fits well with our observations of CO_2 and H_2O emissions at the surface. In Mètrich et al. (2010) (figure 7) and Aiuppa et al. (2010) (figure 7a) CO_2

fluxing is invoked to explain an isobaric decrease in dissolved H_2O from ~3 to ~2 wt% at 200 MPa. Inclusions with 3 wt% water contain up to 1500 ppm CO_2, and calculations with the model of Papale et al. (2006) reveal that the composition of fluid in equilibrium with such a melt contains 61 mol% CO_2 and 39 mol% H_2O, and that this fluid makes up only 0.04 wt% of the system. In order to extract 1 wt% of H_2O from this melt at constant pressure 10 wt% CO_2 must be added to the system, a remarkable amount. The fluid mixture produced by this flushing contains 76 mol% CO_2 and makes up 11 wt% of the system.

Such a process may occur in the case of a single eruption, where large amounts of CO_2 may collect and then flow through shallower magma during ascent, but in a steady state system in order to have this process systematically affecting a large proportion of magma an improbably CO_2-rich gas would be produced at the surface, with a H_2O/CO_2 molar ratio of approximately 0.5. On the contrary, our results clearly indicate a relatively well-constrained range of H_2O/CO_2 ratios between 6 and 20.

Evidence for flushing may perhaps be observed when the CO_2/SO_2 is particularly high, during a temporary dominance of gas flow from depth compared with that produced from the ascending magma column. However, even in the case of June 2010 when we observe CO_2/SO_2 ratios between 10-12 prior to a major explosion, H_2O/CO_2 ratios remain dominated by H_2O, with ratios between 4 and 12, in line with normal degassing. If flushing really were a significant process on Stromboli we should see H_2O/CO_2 ratios less than 1, because as we show above, very large amounts of CO_2 are needed to produce significant isobaric dehydration.

We conclude that the role of CO_2 flushing is probably more limited in scope than that proposed by Métrich et al (2010) and Aiuppa et al. (2010). There is clearly variability in the supply rate of magma to the open-system degassing zone between 100 and 50 MPa, which does produce a wide range of CO_2/SO_2 values as this deeper gas is superimposed on gas escaping from the ascending magma column. However, we see no evidence from H_2O/CO_2 ratios for CO_2 proportions greater than approximately 3 wt%, and this is far lower than that needed to produce the apparently ubiquitous dehydration signature observed in the melt inclusion data suite.

Two main points follow from this observation. Firstly, the model proposed by Aiuppa et al. (2010) in which low crystal content 'blond' magma is transformed into crystal-rich 'brown' magma due purely to CO_2 fluxing-induced dehydration is difficult to sustain in light of our measurements. Given the continuous supply of magma to the near-surface at Stromboli, as evidenced above, it seems much more probable that H_2O exsolution and crystallisation are driven simply by depressurisation as magma ascends to the surface. Secondly, and consequently, it is clear that we do not yet have a coherent, model to explain the MI H_2O-CO_2 composition distribution at Stromboli. It seems likely that unknown dehydration processes are controlling the MI compositions. One candidate process which merits further investigation is the potential role of water diffusion, with no other chemical exchange, from volatile-rich ascending magma into sinking, degassed magma, a modification of the model proposed by Witham (2011). A further question is the degree to which melt inclusions erupted during a major explosion accurately reflect the steady-state magma dynamics of Stromboli, as opposed to purely short-term processes associated with the explosion itself.

4.4 Comparison with MultiGas measurements on Stromboli

The introduction of the ground-breaking MultiGas instruments (Shinohara 2006) on Stromboli (Aiuppa 2008), combined with the automatic network for SO_2 flux measurements (Burton et al. 2008) has greatly increased our knowledge of magmatic degassing and its relationship with major explosions on this volcano (e.g. Aiuppa et al., 2009, 2010, 2011). We compare our results with those published by Aiuppa et al. (2010) in figure 7. Our measurements agree well with those reported from MultiGas, with a somewhat tighter range of H_2O. The distinctly H_2O-rich character of the CC emissions is clearly seen in the Cerberus data, as well as CO_2 fractionation favouring CO_2

emissions from the SWC. The distribution of CO_2/SO_2 seen in both data sets can be clearly attributed to sampling craters with different CO_2 fractionation together with variations in deep magma supply to the open-system transition.

We highlight that increased CO_2/SO_2 ratios are seen at all craters prior to explosions, and it is this general increase in CO_2/SO_2 which has been detected by MultiGas up until now. Our data clearly indicate though that for any given period CO_2/SO_2 ratio changes from between 4 and 10 could potentially be measured by an in-situ MultiGas station, with this variability being driven simply by the wind transporting the plumes emitted from the different crater vents onto the station (figure 7). This process should be kept in mind when interpreting MultiGas data on Stromboli.

4.5 Forecasting major explosions with Cerberus and insights into the explosion source mechanism

The data we have collected to date shows a tantalising vision of the great potential the Cerberus instrument has for forecasting major explosions on Stromboli with unprecedented clarity. The steady, low values detected in September 2009 show what appear to be typical steady-state background values, while the strong increases in CO_2/SO_2 ratio prior to explosions appear to be very clear indicators of imminent explosive activity. Further measurements are obviously required to confirm these observations, and to increase our knowledge of the SO_2/HCl behaviour in particular, with a view to connecting this gas ratio with shallow, water-rich degassing processes such as puffing.

We detected one measurement of decreased CO_2/SO_2 following a notable increasing trend prior to a major explosion in late November at the SWC (see figure 5). While the increasing trend in CO2/SO2 ratios confirms observations reported in Aiuppa et al., 2011, our measurement of a decrease in the CO_2/SO_2 ratio prior to a major explosion is new, and could be a candidate for a short-term precursor to a major explosion, if confirmed in the future. While emphasising that we only have a single data point demonstrating a decrease in CO_2/SO_2 immediately before a major explosion, we highlight that this observation does not fit well with models of foam accumulation and collapse (e.g. Allard et al., 2010), which would instead produce a steady increase in CO_2 flux as the foam collapses, reaching a peak at the moment of explosion.

As described above and in Burton et al. (2007a) the nature of degassing on Stromboli is the superposition of gas which has risen in closed system together with magma to a depth where the open-system degassing to take place. Above this point gas ascends much quicker than magma, and is progressively mixed with gas released from the ascending magma column within the conduit, producing a superposition of gas at the surface.

An increase in CO_2/SO_2 ratio observed at the surface therefore indicates a temporary increase in the amount of magma which is connected to the open-system degassing network, probably due to unsteady supply of magma from the deeper system. Thus, the relatively fast ascent of a magma pocket towards the open system increases the vesicularity of the deep system and permits a larger volume of magma to connect to the open system. The magma loses CO_2-rich gas until the permeability drops, at which point the interconnected bubbles carrying the fast-ascending gas may collapse, creating a gas coalescence event and inducing the rapid ascent of gas and magma from depth which creates a major explosion at the surface. This hypothesis is supported by evidence of a lower permeability in products from the major explosions compared with black scoria products (Polacci et al., 2009). Thus, the rapid drop in the permeability of the deep magmatic system induces a decrease in CO_2-rich gas flux which may be a short-term precursor to a major explosion.

5. Conclusions

Cerberus is a new innovation for the remote measurement of multiple gas sources at the summit of Stromboli volcano. The major new revelation from its first measurements is that the summit craters of Stromboli appear to produce a heterogeneous gas composition. We have investigated the scientific implications of these observations in some detail, comparing them with previously published models and data. Our data has permitted an original model of the geometrical structure of the shallow plumbing system (figure 6). We find that the H_2O-rich nature of degassing from the CC can explain the relatively low porphyricity of products erupted from this crater, and that it is likely that the source for this H_2O-rich gas is the near-surface magma accumulation which supplies the rapid lava effusions that heralded the initial hours of the 2002/03 and 2007 eruptions of Stromboli. Puffing is water-rich, sourced from the shallow magma body and appears to account for not more than approximately one third of the total degassing flux. Moreover, we conclude that CO_2 flushing is unlikely to be a process which has a major role in the Stromboli system, and highlight that alternative explanations for the great variability in H_2O and CO_2 amounts dissolved in melt inclusions are required. Our data confirm MultiGas observations of increases in CO_2/SO_2 ratio prior to major explosions, and present a new observation of decreased CO_2/SO_2 at the SWC immediately before the explosion. We highlight that the heterogeneous composition of gas emitted from the summit craters should be taken into account when interpreting in-situ MultiGas data collected in the summit area. Finally we propose a model of gas flow collapse as a likely source mechanism for major explosions, to explain the decrease in CO_2/SO_2 ratio observed immediately before such events.

6. Acknowledgments

Cerberus was created through a collaborative project between INGV and the Technical University of Hamburg-Harburg, Germany, with funding from the Italian Regione Sicilia project “AQP Sicilia – task V1”. We gratefully acknowledge stimulating discussions regarding the Stromboli system with P. Landi, M. Pompilio, A. Bertagnini and M. Polacci. G. Salerno and S. Giammanco are warmly acknowledged for their generous support during field maintenance of Cerberus.

We thank A. Aiuppa, P. Allard and C. Oppenheimer for careful and thorough reviews which improved the quality and clarity of the manuscript. Completion of this manuscript was facilitated with funding from ERC project CO_2Volc, n. 279802.

References

Aiuppa, A., Inguaggiato, S., McGonigle, A.J.S., O'Dwyer, M., Oppenheimer, C., Padgett, M.J., Rouwet, D., Valenza, M., (2005). H2S fluxes from Mt. Etna, Stromboli, and Vulcano (Italy) and implications for the sulphur budget at volcanoes. Geochim. Cosmochim. Acta 69 (7), 1861–1871.

Aiuppa, A., C. Federico, G. Giudice, G. Giuffrida, R. Guida, S. Gurrieri, M. Liuzzo, R. Moretti, and P. Papale (2009), The 2007 eruption of Stromboli volcano: Insights from real‐time measurements of the volcanic gas plume CO2/SO2 ratio, J. Volcanol. Geotherm. Res., 182, 221–230, doi:10.1016/j.jvolgeores.2008.09.013.

Aiuppa, A, Burton, M., Caltabiano, T., Giudice, G., Guerrieri, S., Liuzzo, M., Murè, F. and Salerno, G. (2010a), Unusually large magmatic CO2 gas emissions prior to a basaltic paroxysm. Geophys. Res. Lett., VOL. 37, L17303, doi:10.1029/2010GL043837, 2010

Aiuppa, A., Bertagnini, A., Métrich, N., Moretti, R., Di Muro, A., Liuzzo, M. and Tamburello, G. (2010b), A model of degassing for Stromboli volcano, Earth and Planetary Science Letters 295 (2010) 195–204.

Aiuppa, A, Burton, M., Allard, P., Caltabiano, T., Giudice, G., Guerrieri, S., Liuzzo, M., and Salerno, G. (2011), First observational evidence for the CO2 – driven origin of Stromboli's major explosions. Solid Earth, 2, 135-142, . 37, L17303, doi:10.5194/se-2-135-2011

Allard, P., Carbonelle, J., Metrich, N., Loyer, H. and Zettwoog, P. (1994). Sulphur output and magma degassing budget of Stromboli volcano. Nature 368; 326-330.

Allard, P., 1997. Endogenous magma degassing and storage at Mount Etna, Geophys. Res. Lett. 24, 2219-2221.

Allard, P., Aiuppa, A., Loyer, H., Carrot, F., Gaudry, A., Pinte, G., Michel, A., Dongarra, G., (2000). Acid gas and metal emission rates during long-lived basalt degassing at Stromboli volcano. Geophys. Res. Lett. 27 (8), 1207–1210.

Allard, P., Burton, M. & Murè, F. (2005). Spectroscopic evidence for a lava fountain driven by previously accumulated magmatic gas. Nature 433; 407-410.

Allard, P., Aiuppa, A., Burton, M., Caltabiano, T., Federico, C., Salerno, G., La Spina, A. (2008). Crater gas emissions and the magma feeding system of Stromboli volcano. In: Learning from Stromboli Volcano: insights from the 2002-2003 eruption, (eds. Calvari, S., Inguaggiato, S., Ripepe, M., Rosi, M.), AGU Geophys. Monograph. Series, vol. 182, Washington DC, 182, Chap. 1.5, 65–80.

Allard, P., (2010), A CO2-rich gas trigger of explosive paroxysms at Stromboli basaltic volcano, Italy. J. Volcanol. Geoth. Res. 189, 363–374.

Andronico, D. and Pistolesi, M. (2010) The November 2009 paroxysmal explosions at Stromboli, J. Volcanol. Geoth. Res. 196, 120–125

Barberi, F., Rosi, M., Sodi, A., (1993), Volcanic hazard assessment at Stromboli based on review of historical data. Acta Vulcanol. 3, 173–187.

Bertagnini, A., Métrich, N., Landi, P., Rosi, M., (2003), Stromboli volcano (Aeolian Archipelago, Italy): an open window on the deep-feeding system of a steady state basaltic volcano. J. Geophys. Res. 10 (B7), 2336. doi:10.1029/2002JB002146.

Bertagnini, A., Métrich, N., Francalanci, L., Landi, P., Tommasini, S., Conticelli, S., (2008), Volcanology and magma geochemistry of the present-day activity: constraints on the feeding system. In: Calvari, S., Inguaggiato, S., Ripepe, M., Rosi, M. (Eds.), The Stromboli Volcano: An Integrated Study of the 2002–2003 Eruption: AGU Geophys. Monograph. Series, Washington DC, vol. 182, pp. 19–37.

Burgisser, A. and Scaillet, B. (2006), redox evolution of a degassing magma rising to the surface, Nature, 445, 194-197, doi:10.1038/nature05509.

Burton, M.R., Remote sensing of the atmosphere using Fourier transform spectrometry, Ph.D. Thesis, Univ. Cambridge, UK, 1999.

Burton, MR; Oppenheimer, C; Horrocks, LA; Francis, PW. 2000. Remote sensing of CO2 and H2O emission rates from Masaya volcano, Nicaragua. Geology, 28 (10): 915-918.

Burton M., P. Allard, F. Murè and C. Oppenheimer (2003). FTIR remote sensing of fractional magma degassing at Mount Etna Sicily, in Volcanic degassing, Geological Society of London Special Publications, 213, pp 281-294, eds. C. Oppenheimer, D. Pyle and J. Barclay.

Burton, M.R., Allard, P., Muré, F., La Spina, A., (2007a), Magmatic gas composition reveals the source depth of slug-driven strombolian explosive activity. Science 37, 227–230.

Burton M.R., Mader H.M., Polacci M., (2007b), The role of gas percolation in quiescent degassing of persistently active basaltic volcanoes, Earth and Planetary Science Letters , 264, 1-2, 46-60

Burton, M.R., Caltabiano, T., Mure, F., Salerno, G., Randazzo, D. (2009), SO_2 flux from Stromboli during the 2007 eruption: Results from the FLAME network and traverse measurements, Journal of Volcanology and Geothermal Research, 182 (3-4): 214-220 Sp. Iss., DOI: 10.1016/j.jvolgeores.2008.11.025

Dixon, J. E., Stolper, E. M. & Clague, D. 1991 Degassing history of water, sulfur, and carbon in submarine lavas from Kilauea Volcano, Hawaii. J. Geol. 99, 371–394.

Duffell, H; Oppenheimer, C; Burton, M. (2001), Volcanic gas emission rates measured by solar occultation spectroscopy, Geophys. Res. Lett., 28 (16): 3131-3134.

Harris, A. and Ripepe, M., (2007), Temperature and dynamics of degassing at Stromboli. J. Geophys. Res. 112, B03205 doi:10.1029/2006JB004393.

Jaupart, C. and Vergniolle, S. (1998), Laboratory models of Hawaiian and Strombolian eruptions. Nature 331, 58–60.

La Felice, S and Landi. P. (2011), The 2009 paroxysmal explosions at Stromboli (Italy): magma mixing and eruption dynamics, Bull Volcanol 73:1147–1154; doi:10.1007/s00445-011-0502-z

Landi, P., Francalanci, L., Pompilio, M., Rosi, M., Corsaro, R.A., Petron, C.M., Nardini, I and Miraglia, L., (2006). The December 2002–July 2003 effusive event at Stromboli volcano, Italy: Insights into the shallow plumbing system by petrochemical studies. J. Volcanol. Geoth. Res. 155, 263–284 doi: 10.1016/j.jvolgeores.2006.03.032

Landi, P., Corsaro, R.A., Francalanci, L., Civetta, L., Miraglia, L., Pompilio, M., Tesoro, R., 2009. Magma dynamics during the 2007 Stromboli eruption (Aeolian islands, Italy): mineralogical, geochemical and isotopic data. J. Volcanol. Geoth. Res. 182,, 255-268. doi: 10.1016/j.jvolgeores.2008.11.010.

Landi, P., Marchetti, E., La Felice, S., Ripepe, M. and Rosi, M. (2011), Integrated petrochemical and geophysical data reveals thermal distribution of the feeding conduits at Stromboli volcano, Italy. Geophys. Res. Lett., VOL. 38, L08305, doi:10.1029/2010GL046296.

La Spina, A., Burton, M. and Salerno, G., (2010), Unravelling the processes controlling gas emissions from the central and northeast craters of Mt. Etna, J. Volcanol. Geotherm. Res. doi:10.1016/j.jvolgeores.2010.09.018

Marquardt D.,(1963), An Algorithm for Least-Squares Estimation of Nonlinear Parameters. SIAM Journal on Applied Mathematics 11 (2): 431–441. doi:10.1137/0111030.

Métrich, N., Bertagnini, A., Landi, P., Rosi, M., (2001), Crystallization driven by decompression and water loss at Stromboli volcano (Aeolian Islands, Italy). J. Petrol. 42, 1471–1490.

Métrich, N., Bertagnini, A., Landi, P., Rosi, M., Belhadj, O., (2005), Triggering mechanism at the origin of paroxysms at Stromboli (Aeolian archipelago, Italy): the 5 April 2003 eruption. Geophys. Res. Lett. 32, L103056 doi:10.1029/2004GL022257.

Métrich, N., Bertagnini, A. and Di Muro, A., (2010), Conditions of magma storage, degassing and ascent at Stromboli: new insights into the volcano plumbing system with inferences on the eruptive dynamics, J. Petrol. 51, 603–626. doi: 10.1093- petrology-egp083.

Oppenheimer, C; Francis, P; Burton, M; Maciejewski, AJH; Boardman, L. (1998), Remote measurement of volcanic gases by Fourier transform infrared spectroscopy. App. Phys. B.-Lasers and Optics, 67 (4): 505-515.

Oppenheimer, C., Lomakina, A.S., kyle, P.R., kingsbury, N.G. and Boichu, M. (2009), Pulsatory magma supply to a phonolite lava lake. Earth Planet. Sci. Lett. doi:10.1016/j.epsl.2009.04.043.

Papale, P., 1999. Modeling of the solubility of a two-component H_2O+CO2 fluid in silicate liquids. Am. Mineral. 84, 477– 492.

Papale, P., Moretti, R. & Barbato, D. (2006). The compositional dependence of the saturation surface of H2O þ CO2 fluids in silicate melts. Chemical Geology 29, 78-95.

Polacci, M., Baker, D.R., Mancini, L., Favretto, S. and Hill, R.J., (2009), Vesiculation in magmas from Stromboli and implications for normal Strombolian activity and paroxysmal explosions in basaltic systems. J. Geophys. Res. 114 art. no. B01206.

Ripepe, M. and Gordeev, E., (1999), Gas bubble dynamics model for shallow volcanic tremor at Stromboli. J. Geophys. Res. 106, 8713–8727.

Rodgers, C., 2000. Inverse Methods For Atmospheric Sounding, Theory and Practice, Series on Atmospheric, Oceanic and Planetary Physics – Vol. 2, edited by F.W. Taylor, World Scientific.

Rosi, M., Bertagnini and A., Landi, P., (2000), Onset of the persistent activity at Stromboli volcano (Italy). Bull. Volcanol. 62, 294–300.

Rothman, L.S., C.P. Rinsland, A. Goldman, S.T. Massie, D.P. Edwards, J.-M. Flaud, A. Perrin, C. Camy-Peyret, V. Dana, J.-Y. Mandin, J. Schroeder, A. McCann, R.R. Gamache, R.B. Wattson, K.Yoshino, K.V. Chance, K.W. Jucks, L.R. Brown, V. Nemtchinov, and P. Varanasi. (1998), The HITRAN Molecular Spectroscopic Database and HAWKS (HITRAN Atmospheric Workstation): 1996 Edition, J. Quant. Spectrosc. Radiat. Transfer, 60, 665-710.

Jaupart, C., Vergniolle, S., (1989), The generation and collapse of a foam layer at the roof of a basaltic magma chamber. J. Fluid Mech. 203, 347–380.

Menand, T. and Phillips, J.C., (2007), Gas segregation in dykes and sills. J. Volcanol. Geotherm. Res. 159, 393–408.

Papale P, Moretti R, Barbato D (2006) The compositional dependence of the saturation surface of H2O + CO2 fluids in silicate melts. Chemical Geology 229, 78-95.

Ripepe, M., Marchetti, E.,Ulivieri, G., (2007), Infrasonic monitoring at Stromboli volcano during the 2003 effusive eruption: insights on the explosive and degassing process of an open conduit system. J. Geophys. Res. 112, B09207. doi:10.1029/2006JB004613.

Shinohara, H., (2008), Excess degassing from volcanoes and its role on eruptive and intrusive activity. Rev. Geophys. 46 doi:10.1029/2007RG000244 RG4005.

Witham, F., Blundy, J., Kohn, S. C., Lesne, P., Dixon, J., Churacov, S.V. and Botchanikov, R. (2011). SolEx: A model for mixed COHSCl-volatile solubilities and exsolved gas compositions in basalt. Compute&Geosciences. Doi: 10.1016/j.cageo.2011.09.021.

Witham, F. (2011), Conduit convection, magma mixing, and melt inclusion trends at persistently degassing volcanoes, Earth Planet. Sci. Lett., dx.doi.org/10.1016/j.epsl.2010.11.017,

Woods, A.W. and Cardoso, S.S.S., (1997), Triggering basaltic volcanic eruptions by bubble– melt separation. Nature 385, 518–520.

Figure and table Captions:

Figure 1: a) map of Aeolian island arc; b) picture of Stromboli; c) zoom of crater area indicating the position of Cerberus (red point) and the active craters (NE – Northeast; C – Central and SW – South vest).

Figure 2: The Cerberus System. 1- the main components of the system: a) the open-path FTIR spectrometer (M4406-S of Midac Corp); b) infrared camera ((Photon 320 of FLIR); c) the scanner mirror; d) cooling ; 2- the external box with two windows see text for details.3- a) A screen of software with a previous of FTIR spectra; b) the crater terrace viewed from infrared camera, the red square is the source point for the FTIR measure; c) a photo of crater terrace.

Figure 3: Intensity of Infrared radiation and CO_2/SO_2 molar ratio collected on 18 November from SW crater (a) and NE crater (b). The peaks and blue diamonds are due to explosive events of “ordinary” activity. We note the compositional difference between the passive degassing and explosive events. White diamonds are the interval considered to characterize the passive degassing.

Figure 4: (a)–(c): Molar ratios of volcanic gas emissions for 19 November 2009; in black from CC, in grey from NEC and in white from SWC; (a) H_2O/SO_2 molar ratio. (b) CO_2/SO_2 molar ratio. (c) HCl /SO_2 molar ratio. The error in the retrieved gas amount is ~5–6% for H_2O, CO_2, SO_2 and HCl.

Figure 5: (a)-(c): Molar ratios trend of volcanic gas phase emitted by active crater in the intervals considered. (a) H_2O/CO_2 molar ratio. (b) CO_2/SO_2 molar ratio. (c) HCl/ SO_2 molar ratio.

Figure 6: Schematic model of the steady-state degassing system on Stromboli revealed by Cerberus measurements. Coloured bars represent degassing fluxes from three sources, as indicated in the legend, and their widths are qualitative indicators for their relative contribution to the combined, final gas output from each crater. The figure begins at the bottom at the point of transition to open-system degassing, with the gas created up to that point indicated as blue. Degassing from ascending magma within the column is red and gradually increases from zero to indicate its progressively greater abundance as function of decreasing pressure. Gas released from the shallow magma accumulation zone is green. The SWC carries the largest contribution of gas produced in closed-system degassing, and is therefore richest in CO_2, while the NEC has the weakest connection to the closed-system gas source, and is therefore relatively poor in CO_2. The branch depth of 30-40 MPa is the minimum depth for which such an CO_2/SO_2 fractionation could occur between the SWC and other craters; any shallower and too much SO_2 is degassed to produce a significant change in composition between the craters (see section 4.2).. Note that in this steady-state system magma is continuously supplied to the uppermost plumbing system, degassing and crystallising as it ascends, as indicated by the transition from orange to black, in a qualitative representation of the change from blond to black magma once plagioclase starts to crystallise in large quantities. The final gas observed from each crater is therefore the superposition of different relative amounts of the three

gas sources: CO_2-rich gas from depth, H_2O-SO_2 rich gas released from the ascending magma in the conduit and H_2O-rich gas released from the shallow accumulation zone, possibly in the form of puffing.

Figure 7: H_2O/CO_2 vs. CO_2/SO_2 scatter plot comparing Cerberus data with results from MultiGas by Aiuppa et al. (2010), see section 4.4.

Table 1: Chemical compositions (molar ratios) with their associated standard error (se) of gases emitted from the SWC, CC and NEC.

Table 2: Relative molar gas compositions from the crater vents. Data collected on 17 November 2009 (a) and on 19 November 2009 (b).

Table 1

a

Date	sample time	$CO_2/SO_2 \pm se$			$H_2O/CO_2 \pm se$			$HCl/SO_2 \pm se$		
2009	GMT	NEC	CC	SWC	NEC	CC	SWC	NEC	CC	SWC
28-Aug	13:55-15:44			5.71 ± 0.67			no data			0.51 ± 0.05
29-Aug	03:30-03:46			5.16 ± 1.00			14.94 ± 4.66			0.48 ± 0.07
01-Sep	10:50-12:50	3.87 ± 1.58			no data			0.95 ± 0.09		
02-Sep	14:50-15:45	3.61 ± 0.74			7.94 ± 2.64			0.63 ± 0.04		
03-Sep	15:03-16:05	3.31 ± 0.96			7.51 ± 4.03			0.68 ± 0.04		
04-Sep	04:00-05:50	3.39 ± 0.86			6.93 ± 1.68			0.53 ± 0.05		
08-Sep	13:00-14:00	2.94 ± 0.95			5.22 ± 3.21			0.65 ± 0.05		
10-Sep	09:40-10:40	2.90 ± 0.65			7.76 ± 1.41			0.44 ± 0.03		
11-Sep	08:50-15:20		2.07 ± 0.18			16.45 ± 3.40			0.43 ± 0.01	
14-Sep	06:20-07:37			5.56 ± 1.67			no data			1.05 ± 0.14
15-Sep	13:25-15:58		3.55 ± 0.43			19.15 ± 1.96			0.49 ± 0.01	

b

Date	sample time	$CO_2/SO_2 \pm se$			$H_2O/CO_2 \pm se$			$HCl/SO_2 \pm se$		
2009	GMT	NEC	CC	SWC	NEC	CC	SWC	NEC	CC	SWC
12-Nov	15.00-17:00		4.39 ± 0.33			16.56 ± 0.84			0.47 ± 0.01	
16-Nov	15:30-16:30	2.17 ± 0.53			8.08 ± 2.72			0.52 ± 0.02		
17-Nov	08:50-15:30	4.26 ± 0.86	5.92 ± 1.00	8.20 ± 0.91	7.40 ± 0.85	15.79 ± 0.96	8.35 ± 0.71	0.54 ± 0.06	0.77 ± 0.03	0.84 ± 0.03
18-Nov	10:03-16:26	5.22 ± 0.34		8.59 ± 1.05	7.82 ± 0.78		5.57 ± 0.57	0.96 ± 0.02		1.03 ± 0.03
19-Nov	09:12-15:55	6.21 ± 1.36	6.60 ± 0.60	9.46 ± 0.77	7.05 ± 0.95	16.10 ± 0.60	8.60 ± 1.00	0.60 ± 0.07	0.70 ± 0.02	0.72 ± 0.02
20-Nov	12:00-15:10	6.94 ± 0.38		4.58 ± 0.41	7.99 ± 0.48		10.64 ± 1.47	0.75 ± 0.02		0.62 ± 0.03
24-Nov	11:50-13:00		6.07 ± 0.61			no data			0.44 ± 0.04	
26-Nov	12:08-13:00	3.22 ± 0.76			21.54 ± 2.14			0.52 ± 0.05		
27-Nov	08:28-14:26		3.73 ± 0.15			19.01 ± 0.79			0.56 ± 0.01	
02-Dec	10:00-10:40	2.24 ± 0.63			17.25 ± 3.25			0.48 ± 0.06		

c

Date	sample time	$CO_2/SO_2 \pm se$			$H_2O/CO_2 \pm se$			$HCl/SO_2 \pm se$		
2010	GMT	NEC	CC	SWC	NEC	CC	SWC	NEC	CC	SWC
27-May	03:15-05:30	3.84 ± 0.80			9.08 ± 2.69			0.49 ± 0.04		
28-May	13:40-15:50	4.36 ± 0.70			8.39 ± 5.58			0.56 ± 0.04		
29-May	07:00-13:46	4.21 ± 0.88			12.81 ± 1.98			0.37 ± 0.03		
30-May	15:00-20:00	3.59 ± 0.98			no data			0.77 ± 0.05		
11-Jun	03:00-03:50			9.95 ± 1.60			no data			0.74 ± 0.09
14-Jun	12:20-14:30	5.57 ± 1.67			6.55 ± 2.90			0.54 ± 0.06		
17-Jun	13:55-17:00	6.79 ± 1.65		9.076 ± 0.71	no data		6.70 ± 1.87	0.46 ± 0.04		0.41 ± 0.05
18-Jun	04:50-10:40	10.40 ± 2.94			13.33 ± 1.28			0.66 ± 0.05		
19-Jun	11:15-13:26	10.04 ± 2.94			4.44 ± 2.69			0.44 ± 0.08		
20-Jun	13:07-16:45	14.50 ± 1.73			no data			0.48 ± 0.04		

Table 2

a

Vent	H_2O %	CO_2 %	SO_2 %	HCl %
NEC	88.28%	8.60%	2.02%	1.10%
CC	92.64%	5.66%	0.96%	0.74%
SWC	85.48%	11.89%	1.45%	1.19%

b

Vent	H_2O %	CO_2 %	SO_2 %	HCl %
NEC	90.01%	7.95%	1.28%	0.76%
CC	94.84%	4.10%	0.62%	0.43%
SWC	88.48%	10.00%	0.88%	0.63%

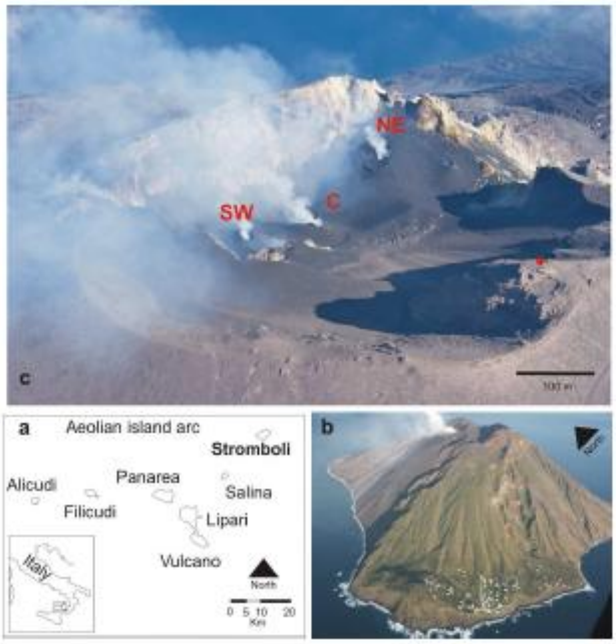

NE
SW
C
c
a
Aeolian island arc
Stromboli
Alicudi
Panarea
Salina
Filicudi
Lipari
Vulcano
Italy
North
0 5 10 20
Km
b
North

Figure 1

Figure 2

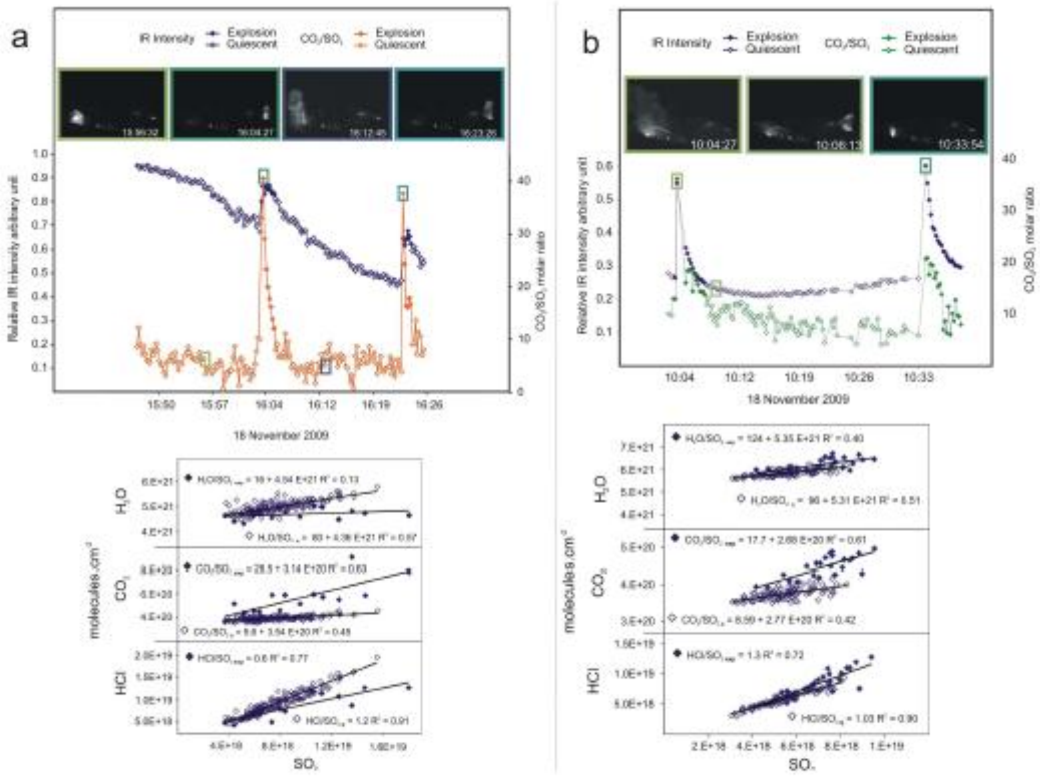

Figure 3

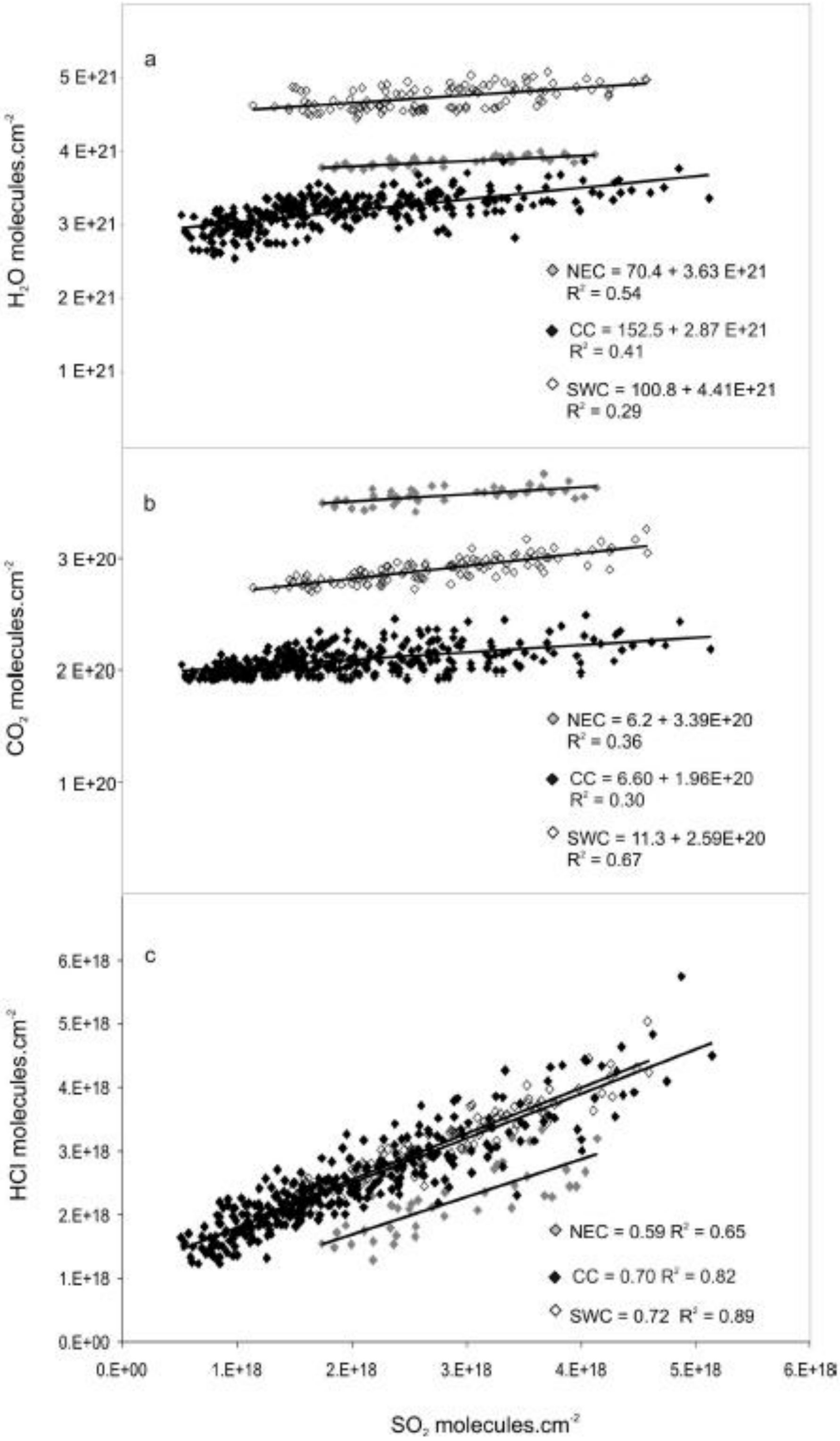

a
5 E+21
4 E+21
3 E+21
2 E+21
1 E+21
H2O molecules.cm-2
NEC = 70.4 + 3.63 E+21
R2 = 0.54
CC = 152.5 + 2.87 E+21
R2 = 0.41
SWC = 100.8 + 4.41E+21
R2 = 0.29
b
3 E+20
2 E+20
1 E+20
CO2 molecules.cm-2
NEC = 6.2 + 3.39E+20
R2 = 0.36
CC = 6.60 + 1.96E+20
R2 = 0.30
SWC = 11.3 + 2.59E+20
R2 = 0.67
c
6.E+18
5.E+18
4.E+18
3.E+18
2.E+18
1.E+18
0.E+00
HCl molecules.cm-2
NEC = 0.59 R2 = 0.65
CC = 0.70 R2 = 0.82
SWC = 0.72 R2 = 0.89
0.E+00
1.E+18
2.E+18
3.E+18
4.E+18
5.E+18
6.E+18
SO2 molecules.cm-2

Figure 4

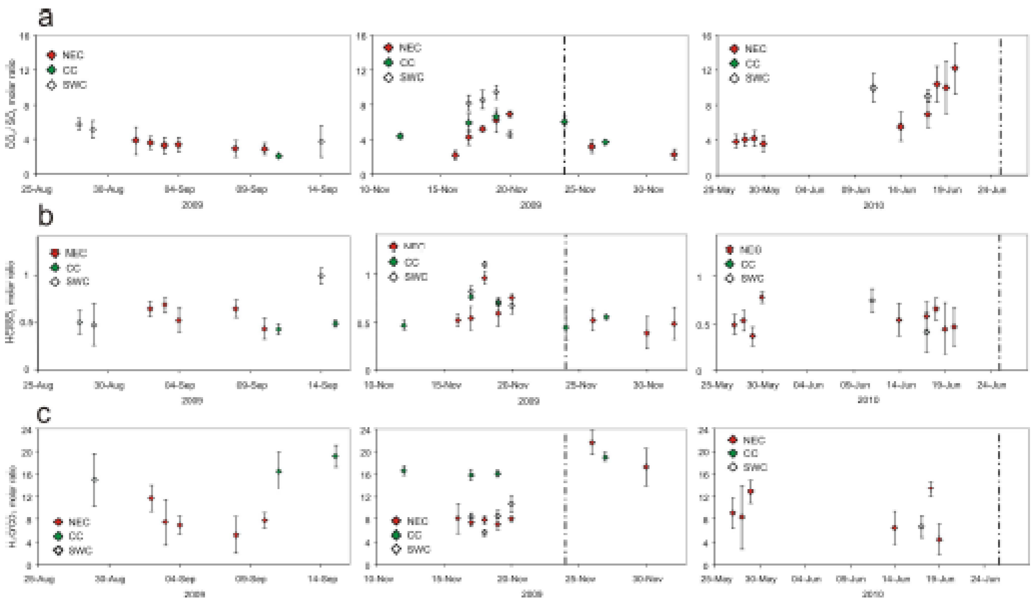

Figure 5

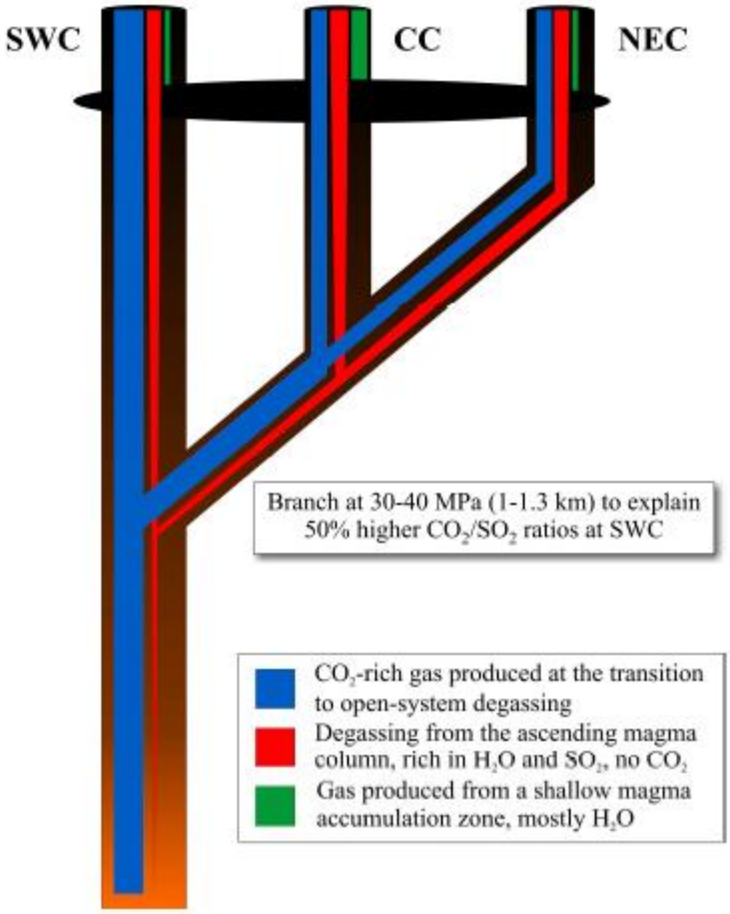
SWC
CC
NEC
Branch at 30-40 MPa (1-1.3 km) to explain 50% higher CO_2/SO_2 ratios at SWC
CO_2-rich gas produced at the transition to open-system degassing
Degassing from the ascending magma column, rich in H_2O and SO_2, no CO_2
Gas produced from a shallow magma accumulation zone, mostly H_2O

Figure 6

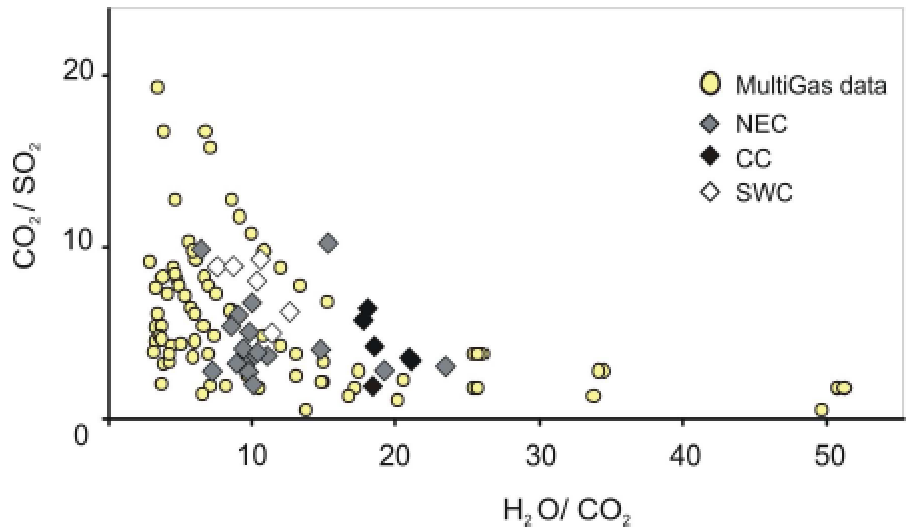

Figure 7

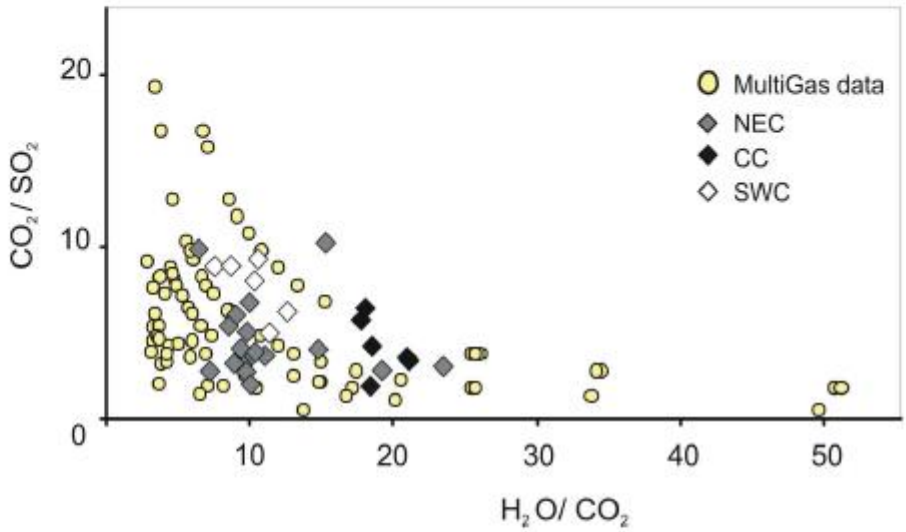

Figure 8

Highlights

A remote-controlled, OP-FTIR scanning system (Cerberus) at the summit of Stromboli

Increase and then decrease in CO_2/SO_2 plume ratios prior to a major explosion.

Gas composition change produces new constraints on explosion-generating mechanism

The collapse of deep permeable network triggers major explosions.